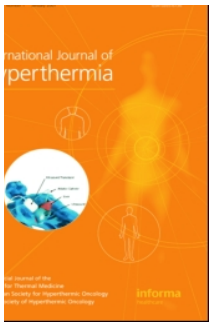

International Journal of Hyperthermia

ISSN: 0265-6736 (Print) 1464-5157 (Online) Journal homepage: http://www.tandfonline.com/loi/ihyt20

A comparison of the heating characteristics of capacitive and radiative superficial hyperthermia

H.P. Kok & J. Crezee

To cite this article: H.P. Kok & J. Crezee (2016): A comparison of the heating characteristics of capacitive and radiative superficial hyperthermia, International Journal of Hyperthermia

To link to this article: http://dx.doi.org/10.1080/02656736.2016.1268726

Accepted author version posted online: 12 Dec 2016.

A comparison of the heating characteristics of capacitive and radiative superficial hyperthermia

H.P. Kok & J. Crezee

Department of Radiation Oncology, Academic Medical Center, University of Amsterdam, Meibergdreef 9, 1105 AZ Amsterdam, The Netherlands.

Keywords: Hyperthermia, RF heating, capacitive heating, hyperthermia treatment planning

Running head: Capacitive vs radiative superficial hyperthermia

Correspondence:
H.P. Kok, PhD
Department of Radiation Oncology,
Academic Medical Center, University of Amsterdam
Meibergdreef 9,
1105 AZ Amsterdam,
The Netherlands.
E-mail : H.P.Kok@amc.uva.nl
Phone : +31-(0)20-5664231
Fax : +31-(0)20-6091278

Abstract

Background: Superficial hyperthermia is applied in combination with radiotherapy for e.g. melanoma and recurrent breast cancer, using both capacitive and radiative systems. In this paper numerical simulations are applied to address the question which technique yields the most favorable heating characteristics.

Methods: A 434MHz contact flexible microstrip applicator (CFMA type 4H, size 19.6×19.6cm^2) and a capacitive system consisting of two circular electrodes with diameter 15 and 25cm were modelled. The water bolus of the CFMA was filled with deionized water and for capacitive heating both saline and deionized water were modelled. Specific absorption rate (SAR) and temperature simulations were performed for a perfused muscle-equivalent phantom and phantoms with a 1cm thick superficial fat layer, assuming cylindrical target regions. Subsequently, a real patient model with a chest wall recurrence was studied with the target assumed to have muscle-like properties, fat properties or heterogeneous properties as derived from the CT Hounsfield Units.

Results: Phantom simulations showed that high SAR peaks occur around the bolus edges with capacitive heating. Power absorption below the fat layer is substantially higher for radiative heating and unless the target region is limited to the fat layer, radiative heating yields better target coverage in terms of SAR and temperature. Patient simulations showed that the T_{90} for radiative heating was 0.4-1.1°C higher compared to capacitive heating.

Conclusion: Radiative heating yields more favorable SAR and temperature distributions for superficial tumors, compared to capacitive heating, especially within heterogeneous tissues. Higher tumor temperatures are achieved without occurrence of treatment limiting hot spots.

Introduction

Hyperthermia, i.e. heating of tumors to temperatures of 41-45°C for 1h, is a proven radiosensitizer and chemosensitizer[1]. Superficial hyperthermia is applied to tumors infiltrating up to 4 cm into tissue. Recurrent and metastatic malignant melanoma and recurrent breast cancer are examples of superficial tumor sites for which the effectiveness of combined radiotherapy and hyperthermia has been proven in randomized clinical trials[2, 3]. The overall complete response rate for recurrent breast cancer increases from 41% to 59% after adding hyperthermia to radiotherapy[3]. For malignant melanomas a 2-year actuarial local tumour control of 28% was reported for radiotherapy alone, which increased to 46% after adding hyperthermia[2].

The increase in clinical outcome realized by adjuvant hyperthermia is correlated to the quality of the hyperthermia treatment, i.e. the thermal dose realized in the target region[4]. The goal temperature during hyperthermia is typically 43°C [5] and the thermal dose achieved is therefore usually expressed as the number of equivalent minutes at 43°C, calculated using the CEM43 formula[6, 7]. Adequate heating equipment is essential to realize an acceptable thermal dose. Both capacitive and electromagnetic radiative hyperthermia systems are used for superficial heating[8-12]. Capacitive systems are more often used in Asian countries, though also increasingly popular in the Western world.

Commercially available capacitive systems are Thermotron RF8 (Yamamoto Vinita Co, Osaka, Japan), Oncotherm (Oncotherm Kft, Budapest, Hungary) and Celsius TCS (Celsius42+ GmbH, Cologne, Germany), operating at a frequency of 8 or 13.56 MHz. During capacitive heating the patient is lying on a treatment table with an embedded electrode with integrated water bolus bag. Another electrode is positioned on the patient and the resulting currents produced by capacitive thermodynamic effects cause heating of the tumor. When different sizes of electrodes are combined, the power distribution is directed to the side of the

smallest electrode[8], so for superficial heating the diameter of the electrode in contact with the tumor should be smaller than the diameter of the other electrode. Radiative antennas induce an electromagnetic field that is coupled into the patient using a water bolus. Examples of commercial radiative superficial systems are the BSD-500 system (Pyrexar Medical, Salt Lake City, USA), the ALBA ON4000 (ALBA Hyperthermia, Rome, Italy) and contact flexible microwave applicators (CFMA) (SRPC Istok, Fryazino, Moscow region, Russia). These radiative systems have an operating frequency of 434 or 915MHz and are positioned contacting the treatment area.

The frequent clinical application of two distinctly different techniques raises the question whether there are differences in heating characteristics between capacitive and radiative systems that lead to clinically relevant differences in heating quality. Hyperthermia treatment planning is a very useful method to analyze the differences between different heating techniques, using numerical simulation of power and temperature distributions[13]. Kok *et al* demonstrated the use of hyperthermia treatment planning to assess the performance of CFMAs[14]. De Bruijne *et al* applied treatment planning to support the selection of the optimal superficial heating technique in non-standard situations, e.g. metallic implants present in the heated region[15]. Kroeze *et al* compared radiative and capacitive hyperthermia for heating deep-seated tumors[16]. However, treatment planning studies comparing radiative and capacitive heating for superficial applications are lacking.

This study applied hyperthermia treatment planning to analyze the differences in heating characteristics between capacitive and radiative superficial hyperthermia. Absorbed power and temperature simulations were first performed for a perfused muscle anatomy and fat-muscle anatomies to analyze the typical heating patterns of both techniques. Cylindrical superficial target regions were defined and the quality of target heating was quantified for both techniques in terms of SAR coverage and temperature. Next, a real application was

evaluated by performing simulations for a patient with a chest wall recurrence using three different sets of tumor properties.

Methods

Simulations for this study were performed using our in-house developed hyperthermia treatment planning software, which uses voxel-based finite difference calculations. The resolution applied for all simulations was 1×1×1 mm^3. The computational volume for the radiative heating was 269×269×159 voxels; for the capacitive system dimensions were 319×319×289 voxels. The definitions of the radiative applicator, electrodes and water boluses were generated using the Generic Object Format[17].

Radiative and capacitive systems

A contact flexible microwave applicator (CFMA) was modelled to represent radiative heating devices. A CFMA typically operates at 434 MHz and consists of two coplanar active electrodes and a shield electrode, with a fluoroplastic substrate in between[18]. The active electrodes are separated by means of a slot of approximately 5 mm. The orientation of the principal electric field is perpendicular to this slot. The microstrip line is excited by a feeding pin of a coaxial cable. CFMAs are available in five different sizes. A CFMA type 4H was modelled, which has dimensions 19.6×19.6 cm^2. The CFMA was modelled in the flat, unbent shape to allow good comparison with the capacitive applicators. Modelling CFMAs has been described extensively by Kok *et al* [19, 20]. In the water bolus deionized water is circulated and the bolus thickness is typically 1 cm[19].

For capacitive heating systems different sizes of electrodes are available, varying between 4 and 30 cm in diameter[8, 21, 22]. For superficial heating the electrode in contact with the tumor should be smaller than the other electrode. Throughout this study we assume

the tumor to be located near the top antenna. The modelled top and bottom electrodes had a diameter of 15 and 25 cm, respectively, and an operating frequency of 13.56 MHz was assumed. The water bolus is filled with circulating saline (0.4% NaCl [8, 23]) or deionized water, depending on the type of capacitive system used, and the bolus thickness is typically 2 cm. A schematic drawing of both heating systems is shown in Fig. 1.

Phantom models

Phantom simulations were performed for three different perfused models to analyze the basic heating properties for radiative and capacitive superficial hyperthermia (see Fig. 1):

- Phantom 1: a muscle-equivalent geometry.
- Phantom 2: a fat-muscle geometry. The fat-layer has a uniform thickness of 1 cm and extends over the full surface of the phantom.
- Phantom 3: a fat-muscle geometry comparable to phantom 2, but in this case the 1 cm thick fat layer covers only half of the phantom surface.

Phantom 1 will allow to compare the basic heating characteristics and phantom 2 and 3 will highlight differences in heating properties when tissue heterogeneities are present. In all three models a central cylindrical superficial target region was defined with a diameter of 10 cm. Both a 1 cm thick and a 2 cm thick target region were modelled .

Patient model

The patient model was derived from a 35 cm CT data set (slice thickness 5 mm, Fig. 2) of a patient with a recurrent breast carcinoma of the chest wall. Segmentation was performed using Hounsfield unit thresholding[24] and the tumor was delineated manually by a physician. The segmented anatomy was rotated and resampled to the modeling resolution such that the CFMA and the top electrode could be modelled as a flat structure, comparable to the

representation in the phantom simulations. Then the anatomy was combined with the model of the CFMA or capacitive electrodes. For the CFMA antenna both an antenna orientation with the electric field in cranial-caudal direction or in left-right direction was modelled. The voxels corresponding to the tumor delineation had a total volume of 13.3 cm^3 and the target region extended to approximately 1.5 cm below the skin. To compare the heating characteristics for capacitive and radiative heating in this patient anatomy three different scenarios were considered. In case one and case two all voxels in the target region were assigned tissue properties of fat or muscle tissue, respectively, yielding a homogeneous target region. In the third case target voxels were assigned tissue properties corresponding to muscle or fat tissue as determined from the Hounsfield unit based segmentation. In this case about 40% of the target corresponded to fatty tissue. The advantage of this extended use of the patient model is that it is very effective in demonstrating which anatomical features of the target region would favor capacitive heating and which radiative heating.

SAR calculations

For radiative heating the electromagnetic field was calculated by solving Maxwell's equations using the finite difference time domain (FDTD) method[25]. A perfectly matched layer boundary condition was applied[26]. From the electromagnetic field E the power density (PD) or specific absorption rate (SAR) can be calculated using

$$\mathrm{PD} = \frac{\sigma}{2}\left\|\vec{E}\right\|^2 = \rho \cdot \mathrm{SAR} \qquad (1)$$

with σ (S m^{-1}) the electric conductivity and ρ (kg m^{-3}) the tissue density.

Because of the low frequency applied for capacitive heating, power distributions were calculated by solving the quasi-static formulation of Maxwell's equations. Kroeze *et al*

demonstrated that this is a valid approach for treatment planning for capacitive hyperthermia[23]. The electric field vector can be written as $\vec{E} = -\nabla V$. This quasi-static formulation yields an elliptic partial differential equation to be solved for the potential V [27]. The electrode plates at the top and bottom were kept at a constant potential of 1V and -1V, respectively. The boundaries of the simulation domain were fixed at zero potential. The dielectric properties used for the simulations were taken from the literature and are listed in Table 1[28, 29].

Temperature calculations

Thermal simulations were performed by solving Pennes' bio heat equation[30]:

$$c\rho \frac{\partial T}{\partial t} = \nabla \cdot (k_{tis} \nabla T) - c_b W_b (T - T_{art}) + PD \quad (2)$$

with c the specific heat capacity (J kg^{-1} °C^{-1}). The first term on the right hand side represents the heat conduction in tissue, with k_{tis} (W m^{-1} °C^{-1}) the thermal conductivity. The second term models the perfusion, with c_b the specific heat capacity of blood, W_b (kg m^{-3} s^{-1}) the volumetric perfusion rate and T_{art} the local arterial or body core temperature. A constant water bolus temperature of 41°C was modelled for both systems. Density and thermal properties were taken from the literature and are listed in Table 2[28, 29]. The muscle tissue corresponding to the target region was assigned half the perfusion of regular muscle tissue. For fat tissue in the target the perfusion was unchanged. Steady state temperatures were calculated with the total absorbed power for each individual situation scaled such that the maximum temperature was 44°C, allowing a fair comparison with the same treatment limiting maximum temperature for each case.

Analysis

For the phantom models absorbed power and temperature distributions were compared for both heating methods. For quantitative analysis of differences in SAR patterns the SAR values averaged over 1cm^3 tissue were calculated and normalized to 100% at the maximum value. This normalization allows a fair comparison with SAR values relative to the treatment limiting maximum value for all cases. Relative SAR profiles were compared at the phantom surface and directly below the fat layer. The percentages of the target volume with a relative SAR value higher than 50% of the maximum were also compared for all cases. The temperature distributions were compared quantitatively by means of the indexed temperatures T_{10}, T_{50} and T_{90} defined as the temperature at least achieved in 10, 50 and 90% of the target volume, respectively.

For the patient models the simulated temperature distributions were compared after scaling the power density such that the maximum temperature is 44°C. A temperature volume histogram was generated for the target region for each situation and the T_{10}, T_{50} and T_{90} were determined.

Results

Phantom simulations

Relative SAR profiles at the surface of the phantom and directly under the fat layer along the lines x=0 and y=0 through the center are shown in Figure 3 (phantom 1 and 2) and Figure 4 (phantom 3). Figure 3 clearly shows that capacitive heating results in high SAR peaks around the bolus edges, due to the high current density near the electrode edges. These SAR peaks are less pronounced when the bolus bag is filled with deionized water instead of saline. Furthermore, it is shown that for radiative heating the power absorption below the fat layer is substantially higher compared to capacitive heating. Figure 4 demonstrates that for phantom 3 heating with a capacitive system yields the maximum SAR in the fat layer, whereas the radiative CFMA has its maximum in muscle tissue. Again, the power absorption below the fat layer is substantially higher for radiative heating compared to capacitive heating.

The percentage of the target volume with a SAR value higher than 50% of the SAR maximum is presented in Figure 5 for all cases. The very high SAR peaks around the bolus edges for capacitive heating with a saline bolus results in 0% of the target region to reach 50% of the maximum SAR for phantom 1 and 3. For phantom 2 the large power absorption in the superficial fat layer explains why capacitive heating has a better SAR coverage for a 1cm deep target region. When the target region extends beyond this superficial fat layer, the radiative antenna generates a higher power absorption in the target. For the majority of the cases the radiative CFMA yields a more favorable SAR coverage.

The indexed temperatures T_{10}, T_{50} and T_{90} corresponding to the simulated temperature distributions for all cases are compared in Figure 6. Overall, radiative heating seems more robust to achieve therapeutic temperatures. Especially for phantom 2 and 3, where the target region extends beyond the fat layer, capacitive heating yields a disappointing T_{90} of around 39°C, both for a bolus filled with saline and deionized water.

Patient simulations

Results for the patient simulations confirm that radiative heating is more robust for adequate target heating. Figure 7 shows temperature volume histograms for the simulated temperature distributions assuming a muscle-like target region, a fatty target region or a heterogeneous target region with tissue properties as derived from the CT Hounsfield Units. For all cases the radiative CFMA with the E-field in left-right direction yields the highest temperatures in the target. In case of a muscle-like target and a heterogeneous target the maximum treatment limiting temperature is in the target region for heating with a CFMA with the E-field in left-right direction, whereas for capacitive heating the maximum temperature is in normal tissue. Figure 8 summarizes the indexed target temperatures T_{10}, T_{50} and T_{90} for these cases. Comparison of the best cases for both capacitive and radiative heating shows that the CFMA yields a T_{90} that is 0.4-1.1°C higher compared to capacitive heating, depending on the tissue properties of the target. For the T50 this difference is 0.3-1.7°C in favor of radiative heating. Figure 9 shows the simulated distributions for a CFMA with the E-field in left-right direction and for capacitive heating with a saline bolus. These distributions clearly demonstrate the better target coverage for radiative heating, most pronounced for a muscle-like and heterogeneous target.

Discussion

Comparison of SAR and temperature distributions in perfused muscle tissue, fat-muscle geometries and a patient anatomy showed that radiative hyperthermia is more favorable for heating of superficial tumor locations in heterogeneous anatomies than capacitive hyperthermia. Especially the relatively large power absorption in fatty tissue during capacitive heating yield large inhomogeneities and can therefore limit realization of therapeutic temperatures in a substantial part of the target. These observations extend the results of Kroeze *et al*, who demonstrated earlier that radiative hyperthermia provides a better heating quality for locoregional hyperthermia of deep-seated tumors, e.g. in the pelvic region, as capacitive heating can yield overheating of superficial fat layers[16]. This overheating can be an important treatment limiting factor and aggressive pre-cooling with water boluses at 5-10°C is often applied with deep locoregional heating to reduce these high temperatures[31], although this cannot always avoid preferential heating at fat-muscle interfaces[32]. Furthermore, for superficial hyperthermia, where the tumor invades the skin, such aggressive cooling is not an option and higher bolus temperatures are applied[8].

The penetration depth of electromagnetic fields decreases with increasing frequency, so the penetration depth of the capacitive device operating at 13.56 MHz is substantially larger than for the radiative CFMA antenna at 434 MHz. Heating of superficially located advanced tumors penetrating 4 cm or more into tissue is a clinical challenge since both the skin surface and the tumor in depth are the target of heating. The large penetration depth of capacitive systems would in principle be very beneficial to heat these tumors at full depth, where standard radiative superficial hyperthermia equipment operating at high frequencies (434-2450 MHz) has an insufficient penetration of the electromagnetic energy. Clinical studies report feasibility of heating bulky tumors with capacitive systems and reported tumor temperatures are in the therapeutic range (40-44°C)[8, 12, 33, 34]. However, clinically

measured temperatures using a limited number of thermometry probes do not provide full information about the 3D temperature distribution and Van Rhoon *et al* reported the need for extensive thermometry to avoid missing hot spots that could lead to subcutaneous burns[32]. Thus, based on the heating characteristics as shown in this paper suboptimal tumor temperatures are still expected in a substantial part of the tumor due to the incidence of treatment limiting normal tissue hot spots, especially in heterogeneous anatomies. This implies that dedicated heating systems are required for superficial, semi-deep and deep-seated tumors.

For the radiative heating in this study CFMAs were modelled that operate at a frequency of 434 MHz. Other radiative systems operating at 915 or 2450 MHz are also clinically applied and have similar power deposition characteristics regarding relative heating of fat and muscle tissue, so general conclusions from this study regarding heating patterns in inhomogeneous anatomies remain valid. However, one should be aware that the effective heating depth is lower for higher frequencies. The effective heating depth has a strong influence on local control rates[35] and clinical performance of higher frequencies is especially good for very superficial tumors, penetrating less than 3 cm in tissue. For example, Van der Zee *et al* showed that for patients with recurrent breast cancer the complete response rate for tumors with a diameter up to 3 cm was comparable at 434 MHz and 2450 MHz (roughly 90%), while for larger tumors the performance of 434 MHz was significantly better than for 2450 MHz and the complete response rate was 65% and 31%, respectively[36]. This underlines the importance to use a heating technique that is appropriate for the tumor site to be treated.

Some capacitive systems use saline bolus bags, where others use deionized water[37]. Although deionized water yields less pronounced SAR peaks around the bolus edges, saline reduces the incidence of normal tissue hot spots for more realistic inhomogeneous situations.

Thus, the cooling medium of the bolus is important for optimization of the capacitive hyperthermia treatment, as demonstrated also in previous studies[37-39]. For example, Brezovich *et al* have shown that the skin toxicity during capacitive heating could be reduced by using a saline bolus of tissue-equivalent conductivity[39]. Despite these steps to optimize capacitive heating, this study has shown that treatment limiting hot spots still remain a clinical issue in heterogeneous anatomies. Radiative heating typically avoids these disadvantages of capacitive heating, since the power absorption in the poorly perfused fat tissue is much lower than in muscle tissue, which produces higher target temperatures without overheating heterogeneous normal tissue.

Clinical studies have shown that tumor control realized by adjuvant hyperthermia is correlated to the target temperatures that can be achieved and especially the minimum temperature T90 is important for clinical outcome[4, 40-42]. For temperatures above 43°C, an increase of 1°C in tumor temperature implies a doubling of the thermal dose, i.e. the cumulative equivalent minutes at 43°C (CEM43)[7]. For temperatures below 43°C, as frequently reported during clinical hyperthermia, the effect is even stronger and a much smaller increase of 0.5°C already yields a doubling of CEM43. The patient simulations in this study showed a T_{90} for radiative heating that is 0.4-1.1°C higher compared to capacitive heating, which implies roughly a factor 2-4 difference in CEM43. Since higher tumor temperatures can be achieved before treatment limiting hot spots occur when using radiative heating in heterogeneous anatomies, clinical use of this technique will benefit clinical results.

Conclusion

This study showed that radiative hyperthermia yields more favorable SAR and temperature distributions for superficial tumor locations, compared to capacitive heating, especially within

heterogeneous tissues. With radiative heating higher tumor temperatures can be achieved without inducing treatment limiting hot spots, which will benefit clinical outcome.

	13.56 MHz		434 MHz	
	σ (S m^{-1})	ε_r (-)	σ (S m^{-1})	ε_r (-)
Air	0	1	0	1
Bone	0.05	30.6	0.09	13.1
Fat	0.03	11.8	0.04	5.6
Fat (target)	0.03	11.8	0.04	5.6
Lung	0.24	95.4	0.38	23.6
Muscle	0.63	138.4	0.81	56.9
Muscle (target)	0.63	138.4	0.81	56.9
Water (deionized)	2.6e-5	73.3	0.026	73.3
Water (saline, 0.4% NaCl)	0.92	72.1	-	-

Table 1: Values of the dielectric properties at 13.56 MHz and 434 MHz used in the simulations; conductivity (σ [S m^{-1}] and relative permittivity (ε_r [-]).

	ρ (kg m^{-3})	c (J kg^{-1} °C^{-1})	k (W m^{-1} °C^{-1})	W_b (kg m^{-3} s^{-1})
Air	1.29	10000*	0.024	0
Bone	1908	1313	0.32	0.12
Fat	888	2387	0.22	1.1
Fat (target)	888	2387	0.22	1.1
Lung	394	3886	0.39	3.6
Muscle	1050	3639	0.56	3.6
Muscle (target)	1050	3639	0.56	1.8
Water (deionized)	1000	4180	6.0	-
Water (saline, 0.4% NaCl)	1000	4180	6.0	-

Table 2: Values of the density and thermal properties used in the simulations; density (ρ [kg m^{-3}]), specific heat capacity (c [J kg^{-1} °C^{-1}]), thermal conductivity (k [W m^{-1} °C^{-1}]) and perfusion (W_b [kg m^{-3} s^{-1}]).* The value of c used for air was ten times too high in order to allow larger time steps in thermal computations. The effect on the steady state temperature is negligible (< $2 \cdot 10^{-5}$ °C).

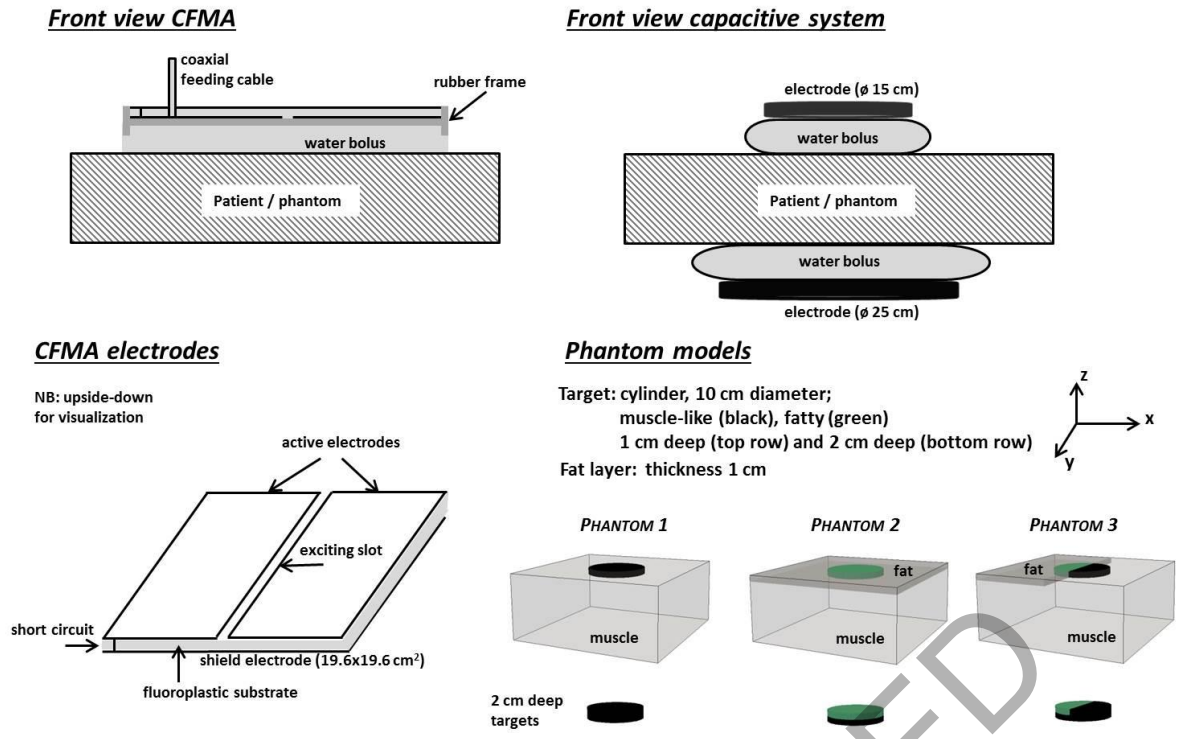

Figure 1: Schematic drawings of the antenna set-up for both systems and the phantom models applied for simulations.

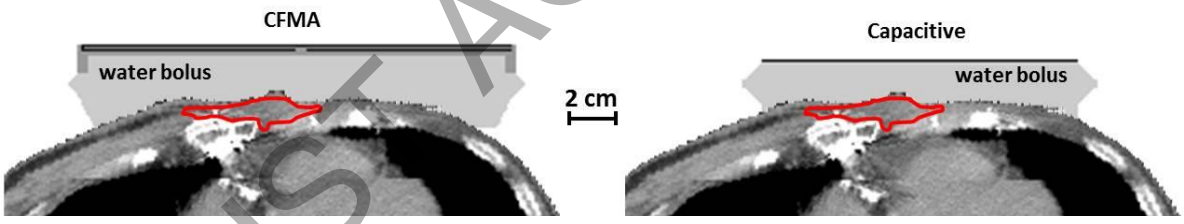

Figure 2: CT scan with the position of the modelled CFMA and capacitive antennas, for a recurrent breast cancer patient model. The red contour represents the target delineation.

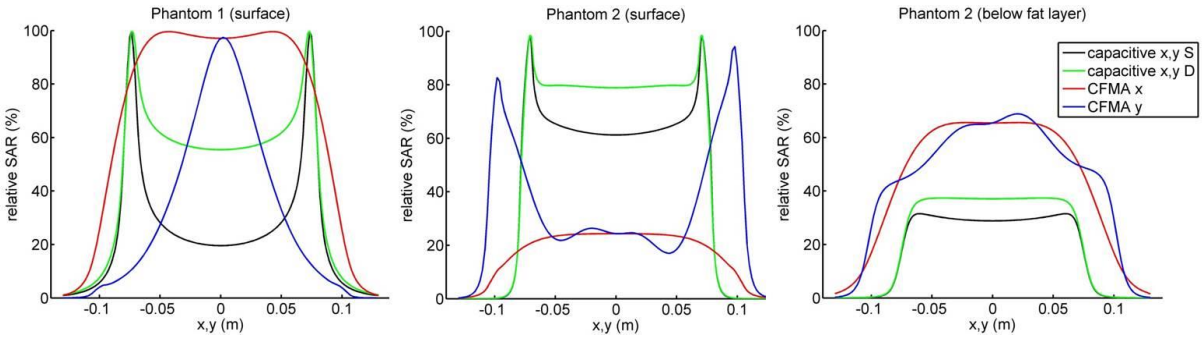

Figure 3: Relative SAR profiles at the surface (phantom 1 and 2) and directly under the fat layer (phantom 2) along the lines x=0 and y=0 through the center. SAR distributions were normalized to 100% at the maximum value anywhere in tissue.

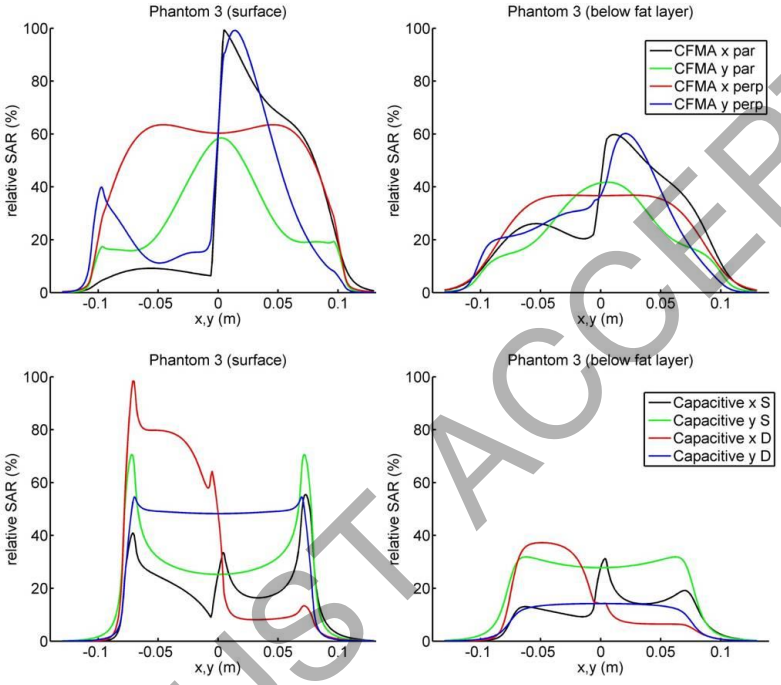

Figure 4: Relative SAR profiles at the surface and directly under the fat layer for phantom 3 along the lines x=0 and y=0 through the center. The top row shows the profiles for the radiative CFMA and the bottom row for capacitive heating. The fat layer covers the part of the phantom with negative x-coordinates. SAR distributions were normalized to 100% at the maximum value anywhere in tissue.

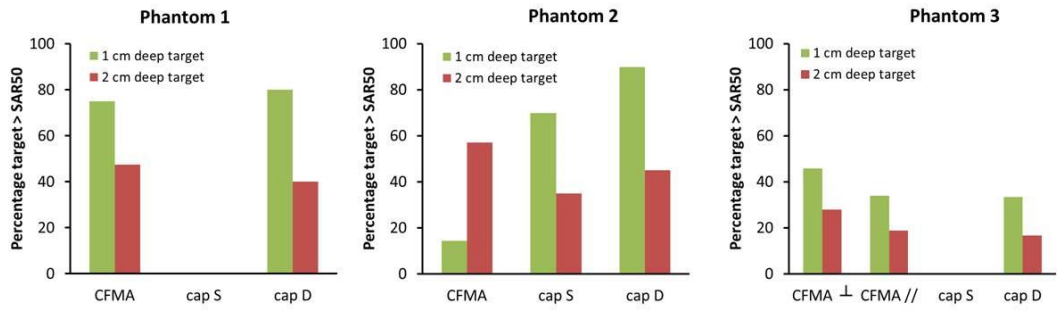

Figure 5: Percentage of the target volume with a SAR value above 50% of the SAR maximum in the phantom, for the three different phantom configurations.

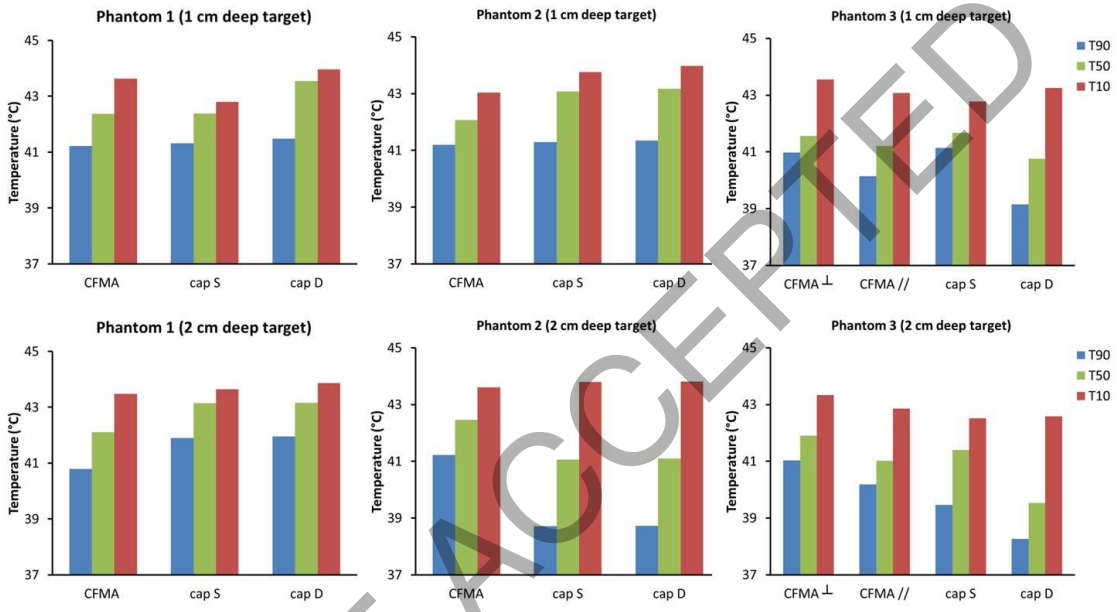

Figure 6: Indexed temperatures T_{10}, T_{50} and T_{90} for the phantom models, assuming a 1 cm deep target (top row) and a 2 cm deep target (bottom row). The total absorbed power was scaled such that the maximum temperature was 44°C.

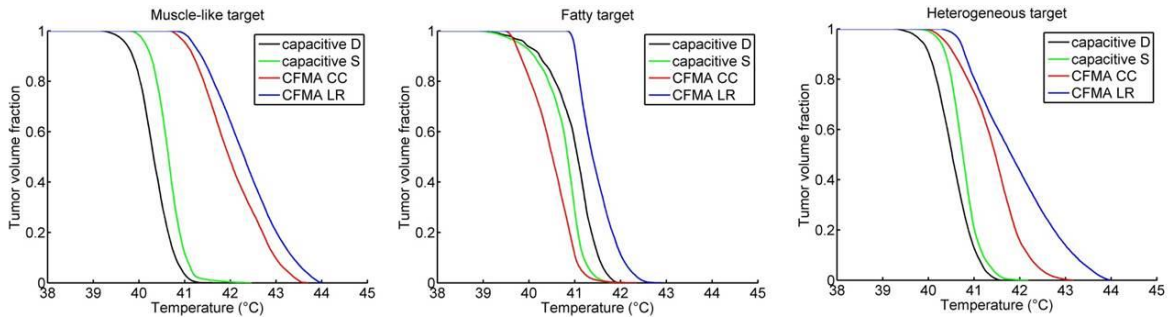

Figure 7: Temperature volume histograms of the delineated target region in a recurrent breast cancer patient. The delineated region was assigned muscle-like tissue properties (left), fatty tissue properties (center) or heterogeneous tissue properties (right) as derived from the CT Hounsfield Units. A deionized water bolus bag for capacitive heating is indicated with 'D', a saline bolus with 'S'. For radiative heating with a 4H CFMA two orientations were modeled: the electric field oriented in cranial-caudal (CC) and in left-right (LR) direction. The total absorbed power was scaled such that the maximum temperature was 44°C.

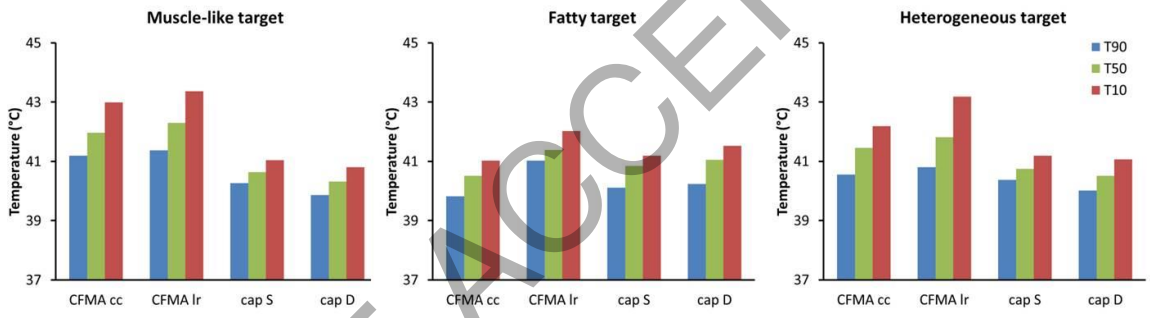

Figure 8: Indexed target temperatures T_{10}, T_{50} and T_{90} simulated for a recurrent breast cancer patient. The delineated region was assigned muscle-like tissue properties (left), fatty tissue properties (center) or heterogeneous tissue properties (right) as derived from the CT Hounsfield units. A deionized water bolus bag for capacitive heating is indicated with 'D', a saline bolus with 'S'. For radiative heating with a 4H CFMA two orientations were modeled: the electric field oriented in cranial-caudal (cc) and in left-right (lr) direction. The total absorbed power was scaled such that the maximum temperature was 44°C.

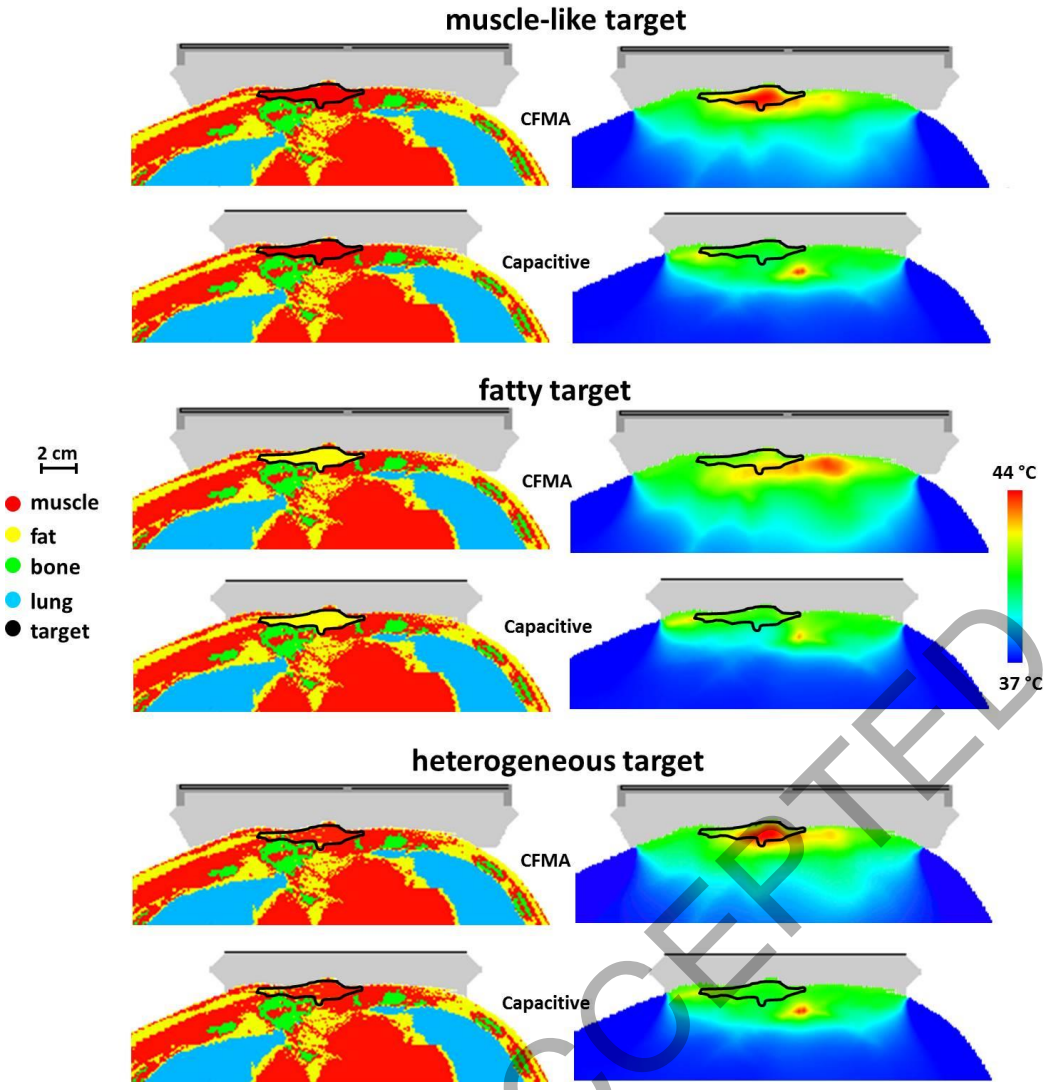

Figure 9: Simulated temperature distributions for capacitive and radiative heating for a patient anatomy, assuming a homogeneous muscle-like target, a homogeneous fatty target or a heterogeneous target with tissue types assigned based on the Hounsfield Units of the CT scan. For capacitive heating the situation with a saline bolus bag is shown and for radiative heating the CFMA was positioned such that the E-field is in left-right direction. The total absorbed power was scaled such that the maximum temperature was 44°C.

References

[1] N. Cihoric, A. Tsikkinis, G. van Rhoon, H. Crezee, D. M. Aebersold, S. Bodis, M. Beck, J. Nadobny, V. Budach, P. Wust, and P. Ghadjar, "Hyperthermia-related clinical trials on cancer treatment within the ClinicalTrials.gov registry," *Int J Hyperthermia,* vol. 31, pp. 609-614, 2015.

[2] J. Overgaard, D. González González, M. C. C. M. Hulshof, G. Arcangeli, O. Dahl, O. Mella, and S. M. Bentzen, "Randomised trial of hyperthermia as adjuvant to radiotherapy for recurrent or metastatic malignant melanoma. European Society for Hyperthermic Oncology," *Lancet,* vol. 345, pp. 540-543, 1995.

[3] C. C. Vernon, J. W. Hand, S. B. Field, D. Machin, J. B. Whaley, J. Van der Zee, W. L. J. van Putten, G. C. Van Rhoon, J. D. P. van Dijk, D. González González, F. F. Liu, P. Goodman, and M. Sherar, "Radiotherapy with or without hyperthermia in the treatment of superficial localized breast cancer: results from five randomized controlled trials. International Collaborative Hyperthermia Group," *Int.J.Radiat.Oncol.Biol.Phys.,* vol. 35, pp. 731-744, 1996.

[4] M. de Bruijne, B. van der Holt, G. C. van Rhoon, and J. van der Zee, "Evaluation of CEM43 degrees CT90 thermal dose in superficial hyperthermia: a retrospective analysis," *Strahlenther Onkol,* vol. 186, pp. 436-43, 2010.

[5] S. A. Sapareto and W. C. Dewey, "Thermal dose determination in cancer therapy," *Int.J.Radiat.Oncol.Biol.Phys.,* vol. 10, pp. 787-800, 1984.

[6] J. W. Hand, J. J. Lagendijk, J. Bach Andersen, and J. C. Bolomey, "Quality assurance guidelines for ESHO protocols," *Int.J.Hyperthermia,* vol. 5, pp. 421-428, 1989.

[7] G. C. van Rhoon, "Is CEM43 still a relevant thermal dose parameter for hyperthermia treatment monitoring?," *Int J Hyperthermia,* vol. 32, pp. 50-62, 2016.

[8] M. Abe, M. Hiraoka, M. Takahashi, S. Egawa, C. Matsuda, Y. Onoyama, K. Morita, M. Kakehi, and T. Sugahara, "Multi-institutional studies on hyperthermia using an 8-MHz radiofrequency capacitive heating device (Thermotron RF-8) in combination with radiation for cancer therapy," *Cancer*, vol. 58, pp. 1589-95, 1986.

[9] P. Gabriele, T. Ferrara, B. Baiotto, E. Garibaldi, P. G. Marini, G. Penduzzu, V. Giovannini, F. Bardati, and C. Guiot, "Radio hyperthermia for re-treatment of superficial tumours," *Int J Hyperthermia*, vol. 25, pp. 189-98, 2009.

[10] E. Puric, J. Heuberger, N. Lomax, O. Timm, and S. Bodis, "The Benefit of Thermoradiotherapy in the Treatment of Superficially Localized Tumors: Experience with Bsd 500 Microwave Hyperthermia System," *Strahlentherapie Und Onkologie*, vol. 185, pp. 648-648, 2009.

[11] S. Oldenborg, V. Griesdoorn, R. van Os, Y. H. Kusumanto, B. S. Oei, J. L. Venselaar, P. J. Zum Vorde Sive Vording, M. W. Heymans, M. W. Kolff, C. R. Rasch, H. Crezee, and G. van Tienhoven, "Reirradiation and hyperthermia for irresectable locoregional recurrent breast cancer in previously irradiated area: Size matters," *Radiother Oncol*, vol. 117, p. 223, 2015.

[12] S. Masunaga, M. Hiraoka, M. Takahashi, S. Jo, K. Akuta, Y. Nishimura, Y. Nagata, and M. Abe, "Clinical results of thermoradiotherapy for locally advanced and/or recurrent breast cancer--comparison of results with radiotherapy alone," *Int J Hyperthermia*, vol. 6, pp. 487-97, 1990.

[13] H. P. Kok, P. Wust, P. R. Stauffer, F. Bardati, G. C. van Rhoon, and J. Crezee, "Current state of the art of regional hyperthermia treatment planning: a review," *Radiat Oncol*, vol. 10, p. 196, 2015.

[14] H. P. Kok, M. De Greef, N. Van Wieringen, D. Correia, M. C. C. M. Hulshof, Z. V. S. V. P.J., J. Sijbrands, A. Bel, and J. Crezee, "Comparison of two different 70 MHz

applicators for large extremity lesions: simulation and application," *Int.J.Hyperthermia*, vol. 26, pp. 376-388, 2010.

[15] M. de Bruijne, D. H. Wielheesen, J. Van der Zee, N. Chavannes, and G. C. Van Rhoon, "Benefits of superficial hyperthermia treatment planning: five case studies," *Int.J.Hyperthermia*, vol. 23, pp. 417-429, 2007.

[16] H. Kroeze, M. Kokubo, J. B. van de Kamer, A. A. C. De Leeuw, M. Kikuchi, M. Hiraoka, and J. J. W. Lagendijk, "Comparison of a Capacitive and a Cavity Slot Radiative applicator for Regional Hyperthermia.," *Japanese Journal of Hyperthermic Oncology*, vol. 18, pp. 75-91, 2002.

[17] J. De Bree, "A 3-D anatomy based treatment planning system for interstitial hyperthermia. PhD Thesis; Utrecht University.," 1998.

[18] E. A. Gelvich and V. N. Mazokhin, "Contact flexible microstrip applicators (CFMA) in a range from microwaves up to short waves," *Ieee Transactions on Biomedical Engineering*, vol. 49, pp. 1015-1023, 2002.

[19] H. P. Kok, M. De Greef, D. Correia, P. J. Zum Vörde Sive Vörding, G. Van Stam, E. A. Gelvich, A. Bel, and J. Crezee, "FDTD simulations to assess the performance of CFMA-434 applicators for superficial hyperthermia.," *Int.J.Hyperthermia*, vol. 25, pp. 462-476, 2009.

[20] H. P. Kok, D. Correia, M. De Greef, G. Van Stam, A. Bel, and J. Crezee, "SAR deposition by curved CFMA-434 applicators for superficial hyperthermia: Measurements and simulations.," *Int.J.Hyperthermia*, vol. 26, pp. 171-184, 2010.

[21] Oncotherm, "http://www.oncotherm.com/," 2016.

[22] Celsius42+, "http://www.celsius42.de/," 2016.

[23] H. Kroeze, J. B. van de Kamer, A. A. de Leeuw, M. Kikuchi, and J. J. Lagendijk, "Treatment planning for capacitive regional hyperthermia," *Int J Hyperthermia,* vol. 19, pp. 58-73, 2003.

[24] S. N. Hornsleth, O. Mella, and O. Dahl, "A new segmentation algorithm for finite difference based treatment planning systems," in *Hyperthermic Oncology 1996 vol. 2*, C. Franconi, G. Arcangeli, and R. Cavaliere, Eds., ed Rome, Italy Tor Vergata, 1996, pp. p. 521-523.

[25] A. Taflove and S. C. Hagness, *Computational Electrodynamics, 2nd edition*, 2nd ed. (Boston, London: Artech House), 2000.

[26] J. P. Berenger, "A Perfectly Matched Layer for the Absorption of Electromagnetic-Waves," *Journal of Computational Physics,* vol. 114, pp. 185-200, 1994.

[27] J. de Bree, J. F. van der Koijk, and J. J. W. Lagendijk, "A 3-D SAR model for current source interstitial hyperthermia," *IEEE Trans.Biomed.Eng*, vol. 43, pp. 1038-1045, 1996.

[28] S. Gabriel, R. W. Lau, and C. Gabriel, "The dielectric properties of biological tissues: II. Measurements in the frequency range 10 Hz to 20 GHz," *Phys.Med.Biol.*, vol. 41, pp. 2251-2269, 1996.

[29] ESHO Taskgroup Committee, "Treatment Planning and Modelling in Hyperthermia, a Task Group Report of the European Society for Hyperthermic Oncology (Rome, Italy: Tor Vergata)," 1992.

[30] H. H. Pennes, "Analysis of tissue and arterial blood temperatures in the resting human forearm. 1948," *J.Appl.Physiol*, vol. 1, pp. 93-122, 1948.

[31] J. G. Rhee, C. K. Lee, J. Osborn, S. H. Levitt, and C. W. Song, "Precooling prevents overheating of subcutaneous fat in the use of RF capacitive heating," *Int J Radiat Oncol Biol Phys,* vol. 20, pp. 1009-15, 1991.

[32] G. C. van Rhoon, J. van der Zee, M. P. Broekmeyer-Reurink, A. G. Visser, and H. S. Reinhold, "Radiofrequency capacitive heating of deep-seated tumours using pre-cooling of the subcutaneous tissues: results on thermometry in Dutch patients," *Int J Hyperthermia,* vol. 8, pp. 843-54, 1992.

[33] N. G. Huilgol, S. Gupta, and R. Dixit, "Chemoradiation with hyperthermia in the treatment of head and neck cancer," *Int J Hyperthermia,* vol. 26, pp. 21-5, 2010.

[34] G. Li, M. Mitsumori, M. Ogura, N. Horii, S. Kawamura, S. Masunaga, Y. Nagata, and M. Hiraoka, "Local hyperthermia combined with external irradiation for regional recurrent breast carcinoma," *Int J Clin Oncol,* vol. 9, pp. 179-83, 2004.

[35] R. J. Myerson, C. A. Perez, B. Emami, W. Straube, R. R. Kuske, L. Leybovich, and D. Von Gerichten, "Tumor control in long-term survivors following superficial hyperthermia," *Int J Radiat Oncol Biol Phys,* vol. 18, pp. 1123-9, 1990.

[36] J. van der Zee, B. van der Holt, P. J. Rietveld, P. A. Helle, A. J. Wijnmaalen, W. L. van Putten, and G. C. van Rhoon, "Reirradiation combined with hyperthermia in recurrent breast cancer results in a worthwhile local palliation," *Br J Cancer,* vol. 79, pp. 483-90, 1999.

[37] N. M. Reddy, V. Shanta, and S. Krishnamurthi, "On minimisation of toxicity to skin during capacitive radio-frequency hyperthermia," *Br J Radiol,* vol. 59, pp. 1129-31, 1986.

[38] H. Griffiths, A. Ahmed, and C. W. Smith, "Power loss in skin cooling pillows during RF hyperthermia," *Br J Radiol,* vol. 57, pp. 254-6, 1984.

[39] I. A. Brezovich, M. B. Lilly, J. R. Durant, and D. B. Richards, "A practical system for clinical radiofrequency hyperthermia," *Int J Radiat Oncol Biol Phys,* vol. 7, pp. 423-30, 1981.

[40] M. Sherar, F. F. Liu, M. Pintilie, W. Levin, J. Hunt, R. Hill, J. W. Hand, C. C. Vernon, G. C. Van Rhoon, V. d. Z. J., D. González González, J. D. P. van Dijk, J. Whaley, and D. Machin, "Relationship between thermal dose and outcome in thermoradiotherapy treatments for superficial recurrences of breast cancer: data from a phase III trial," *Int.J.Radiat.Oncol.Biol.Phys.*, vol. 39, pp. 371-380, 1997.

[41] J. R. Oleson, T. V. Samulski, K. A. Leopold, S. T. Clegg, M. W. Dewhirst, R. K. Dodge, and S. L. George, "Sensitivity of hyperthermia trial outcomes to temperature and time: implications for thermal goals of treatment," *Int.J.Radiat.Oncol.Biol.Phys.*, vol. 25, pp. 289-297, 1993.

[42] K. A. Leopold, M. W. Dewhirst, T. V. Samulski, R. K. Dodge, S. L. George, J. L. Blivin, L. R. Prosnitz, and J. R. Oleson, "Cumulative Minutes with T(90) Greater Than Tempindex Is Predictive of Response of Superficial Malignancies to Hyperthermia and Radiation," *International Journal of Radiation Oncology Biology Physics*, vol. 25, pp. 841-847, 1993.